Influence of decomposition time and H$_2$ pressure on properties of unsupported ammonium tetrathiomolybdate-derived MoS$_2$ catalysts

Jamie Whelan[1,2], Ionut Banu[3], Gisha E Luckachan[1], Nicoleta Doriana Banu[1,4], Samuel Stephen[1], Anjana Tharalekshmy[1], Saleh Al Hashimi[1], Radu V Vladea[1], Marios S Katsiotis[1] and Saeed M Alhassan[1*]

Abstract

Background: Molybdenum sulfide (MoS$_2$) catalysts to be used for hydrodesulfurization (HDS) processes were prepared via the reductive thermal decomposition of ammonium tetrathiomolybdate at fixed temperature (653 K) by varying decomposition times and H$_2$ pressures. Both parameters were found to strongly influence textural and catalytic properties of the resulting MoS$_2$ catalysts.

Methods: Nitrogen sorption, FT-IR, and XRD analyses revealed the effect of varying decomposition times (3 to 7 h) and H$_2$ pressure (20 to 1,000 psig) on the morphology and structure of the catalysts. Dibenzothiophene (DBT) was used to assess catalytic efficiency for HDS reactions.

Results: The influence of time on specific surface was minimal at low pressures but increased at higher decomposition pressures. Vibrational energies of Mo-S bonds in FT-IR indicate that MoS$_2$ catalysts prepared at higher pressures exhibit weaker Mo-S bonds. Analysis of XRD patterns point towards an increase in stacking and crystallite size with increasing pressure; interlayer rotation about both the *a*- and *c*-axes of the stacks was also observed. Catalytic testing results show that conversion increases at higher values of decomposition time and pressure. Partially hydrogenated products were also observed at higher pressures, and the ratio of partially to fully hydrogenated DBT was calculated as an additional measure of catalytic efficiency.

Conclusions: Decomposition time and H$_2$ pressure during ammonium tetrathiomolybdate (ATM) thermal decomposition have a significant impact on the morphological and catalytic properties of the derived MoS$_2$ catalysts. Samples prepared for 5 h at 1,000 psig exhibited the highest conversion of DBT and the lowest ratio of partially to fully hydrogenated products.

Keywords: Ammonium tetrathiomolybdate; MoS$_2$; Hydrodesulfurization; Reductive decomposition pressure

Background

With environmental concerns continually on the rise, greater demand for fuels with low-sulfur content has increased the focus on hydrotreating (HDT) catalysts (Topsøe et al. 1996). Molybdenum sulfide (MoS$_2$)-based catalysts, varyingly promoted with cobalt or nickel, are one of the most common metal sulfides used in HDT, with a strong emphasis on hydrodesulfurization (HDS) reactions (Brunet et al. 2005; Egorova and Prins 2006;

Álvarez et al. 2008; Breysse et al. 2008; Chianelli et al. 2009; Klimov et al. 2010). There are several common methods to synthesize this catalyst such as the direct sulfidation of molybdenum oxide, hydrothermal and sono-chemical synthesis, and the relatively simple procedure of thermally decomposing ammonium tetrathiomolybdate (ATM) (Camacho-Bragado et al. 2005; Devers et al. 2002; Mdleleni et al. 1998; Afanasiev 2008; Polyakov et al. 2008).
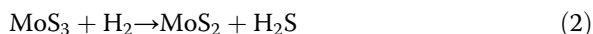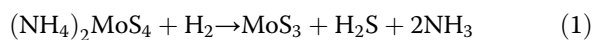
Thermal decomposition of ATM is generally a solid-state reaction and, like similar reactions, can be influenced by a number of different experimental parameters such as temperature, gaseous environment, time, and pressure. The proposed reaction mechanism is a two-step process,

* Correspondence: salhassan@pi.ac.ae
[1]Department of Chemical Engineering, The Petroleum Institute, P.O. Box 2533, Abu Dhabi, United Arab Emirates
Full list of author information is available at the end of the article

Whelan *et al. Journal of Analytical Science and Technology* (2015) 6:8

Page 2 of 8

as can be shown below as Reactions 1 and 2 (Walton et al. 1998):

$$(NH_4)_2MoS_4 + H_2 \rightarrow MoS_3 + H_2S + 2NH_3 \qquad (1)$$

$$MoS_3 + H_2 \rightarrow MoS_2 + H_2S \qquad (2)$$

While several studies of note have already examined the effect of pre-treatment of ATM and the correlation between MoS_2 HDS activity by varying gaseous environment (e.g., H_2S/H_2) and Mo precursors as well as reducing and sulfiding conditions, little work has focused on the influence of decomposition pressure (Liang et al. 1986; Zhang and Vasudevan 1995; Alonso et al. 1998; Afanasiev 2010). As a general rule, pressure increases are known to decrease the rate of thermal decomposition; however, other influences have been observed. In their study of nitramine compounds, Piermarini et al. found a change in decomposition mechanism above a certain pressure (Piermarini et al. 1987). In addition, Criado et al. studied the decomposition of $CaCO_3$ and observed a shift towards higher decomposition temperatures with increasing CO_2 pressure (Criado et al. 1995).

Though some examples in literature report pressure-induced effects on MoS_2 properties such as electrical conductivity and critical current density, little is known regarding the pressure effects on decomposition of ATM and HDS activity of unsupported MoS_2 catalyst (Sánchez et al. 2006; Alekseevskii et al. 1977). While it could be argued that the impact of decomposition may be small relative to other 'stronger' experimental parameters, clearly, the studies on decomposition of nitramine compounds and $CaCO_3$ show it to be a potentially fruitful exercise. Thus, the present study focuses on pressure and time effects on reductive thermal decomposition of ATM and the catalytic activity of the resulting MoS_2. It is shown that by varying the decomposition parameters, resulting structural and chemical differences prove insightful towards designing an economical catalyst for the effective removal of sulfur. The degree of influence these experimental parameters have on the morphology and activity of MoS_2 catalysts is described below.

Methods
Reagents and solutions
The following chemicals were used as purchased: ATM (Aldrich, Dorset UK, 99.97%), dibenzothiophene (DBT) (Aldrich, 98%), hexadecane (Aldrich, 99%), hydrogen gas (Air Products, 99.992%), and nitrogen gas (Air Products, Allentown, PA, USA; 99.995%).

Catalyst preparation
Ammonium tetrathiomolybdate was weighted on an aluminum boat and placed into a 300-cm^3 batch reactor at room temperature. The reactor was sealed, flushed with N_2 and H_2, and then heated to 623 K (10 K min^{-1}). Upon reaching the reaction temperature, H_2 was injected into the reactor at the required pressure, taken as time zero. After the chosen heating duration was completed, heating would be stopped and the reactor would be allowed to cool naturally while maintaining a reductive (H_2) atmosphere. Upon reaching room temperature, the reactor was degassed, flushed with N_2, opened, and the resulting product (MoS_2) was removed and weighted. Immediately afterwards, the specimen was ground using a pestle and mortar and used for characterization and HDS testing. MoS_2 specimens prepared by this method were named as follows: number (time in hours)-number (hydrogen pressure, psig); decomposition times were 3, 5, and 7 h and H_2 pressures were 20 (0.138 MPa), 500 (3.447 MPa), and 1,000 psig (6.895 MPa). For example, 3-1,000 implies MoS_2 prepared from ATM thermally decomposed at 623 K for 3 h at 1,000 psig H_2.

Characterization
Textural characterization was carried out on all catalysts with N_2 sorption at 77 K with a Quantachrome Autosorb-1 (Quantachrome Instruments, Boynton Beach, FL, USA). Prior to analysis, each sample was degassed under vacuum at 573 K for 2 h; the BET surface area (S_{BET}) was determined from the resulting isotherm. FT-IR spectra were obtained using diffuse reflectance infrared Fourier transform (DRIFT) spectroscopy on a Bruker Vertex 70 (Bruker AXS, Inc., Madison, WI, USA). The dark-colored catalysts were mixed with KBr at a ratio MoS_2:KBr = 1:100 to improve infrared transmission; spectra were collected in the 4,000 to 350-cm^{-1} range. Samples for XRD were mounted on a zero background holder, and spectra were collected with a X'Pert PRO Panalytical Powder diffractometer (PANalytical, Almelo, The Netherlands), using Cu Kα radiation (45 kV and 40 mA) in the 2-theta range 10° to 80° with a step time of 0.01 s. Temperature-programmed reduction (TPR) analyses were carried out under continuous H_2 flow (5% H_2 in He) in a quartz cell at 10 K min^{-1} using a Quantachrome ChemBET 3000 (Quantachrome Instruments, Boynton Beach, FL, USA) coupled with a Hiden Analytical HPR 20 QIC mass spectrometry detector (Hiden Analytical, Warrington, UK). It should be mentioned that in no case was any specimen exposed to air for more than 2 min, thus avoiding oxidation of the sulfide catalysts.

Activity measurements
Freshly synthesized and ground MoS_2 (0.050 g, 3.1×10^{-4} mol) was added to a 100-cm^3 batch reactor. Feedstock used was 1% DBT in hexadecane (25 cm^3). The reactor was sealed, flushed with N_2, and then heated to 573 K under stirring (1,000 rpm). Upon reaching the reaction temperature, H_2 (500 psig) was injected

Whelan *et al. Journal of Analytical Science and Technology* (2015) 6:8

Page 3 of 8

into the reactor (time zero). Heating and stirring would be stopped after 3 h, and the reactor would be left to cool naturally, while retaining a reductive (H_2) atmosphere. Upon reaching room temperature, the reactor was degassed and a sample of the reaction mixture was removed, centrifuged, and the supernatant diluted and analyzed on a gas chromatograph coupled with a sulfur chemiluminescence detector (GC-SCD - Agilent 6C 6980 and SCD 335 (Agilent Technologies, Inc., Santa Clara, CA, USA)). The column was 100% dimethylpolysiloxane, 30 m × 0.32 mm × 1 μm, with a maximum temperature of 598 K. In this study, conversion of DBT was calculated based on the decrease in DBT signal (and increase in partially hydrogenated DBT (HYD)) from the GC-SCD compared to the initial concentration following calibration.

Results and discussion

TPR-MS experiments (Figure 1) show two peaks for the reductive thermal decomposition of ATM in H_2, supporting the proposed ATM decomposition mechanism. Thus, the peak at 475 K is assigned to Reaction (1), the release of H_2S and NH_3 (m/z peaks followed were 16, 17, 32, 33, and 34 amu; for display purposes, only molecular ion peaks are shown), while the peak at 613 K is assigned to Reaction (2), i.e., the release of the second molecule of H_2S.

According to the reaction mechanism, for every mole of ATM that decomposes, four moles of gaseous products are produced ($2NH_3$ and $2H_2S$). Based on the starting concentration of ATM, it was calculated that there was a pressure increase of approximately 15 psig above the H_2 injected upon reaching decomposition temperature; no attempt was made to correct for this during catalyst preparation. In general, throughout this paper, the H_2 decomposition pressures applied are termed as low

(20 psig), medium (500 psig), and high (1,000 psig), and it is only against the pressure trend that meaningful conclusions are obtained, not the actual value itself. It should be noted that the actual pressure 'felt' by the ATM is not exactly the same pressure as mentioned above; variation of pressure around the decomposition reaction zone lead to different values than the set point of the external pressure regulator.
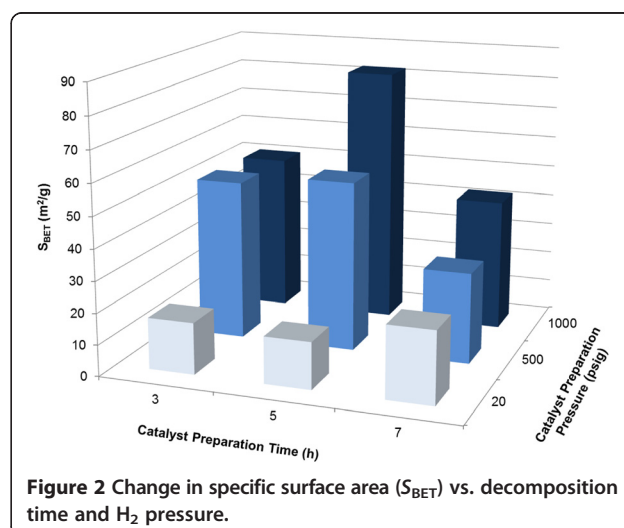
Textural characterization

Textural characterization of the catalysts shows a change in S_{BET} (Figure 2) and total pore volume (TPV) (Figure 3) as a function of decomposition time and pressure, respectively. In general, catalysts prepared at low pressure (20 psig) and low decomposition time (<5 h) exhibited little change in morphology; however, with an increase in pressure, the influence of heating time also increased. Within each time series, increasing pressure resulted in increasing S_{BET} and TPV with the largest changes observed for the 5-h series.
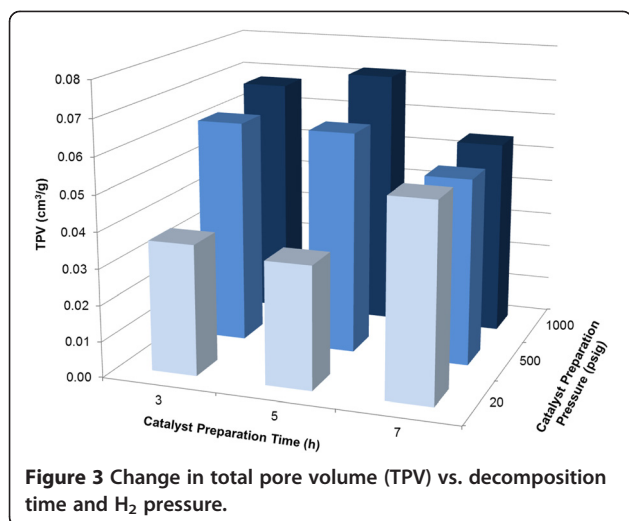
XRD characterization

All samples display the typical diffraction profile for poorly crystalline MoS_2, namely the diffraction peaks of (002), (100), (103), (105), and (110). For the sake of article space, only spectra from specimens prepared at 1,000 psig are shown in Figure 4; all spectra can be found in the Additional file 1. Using the Debye-Scherrer equation applied to the broadening of the (110) diffraction peak, it was found that over time there was an increase in crystalline order along the basal direction, likewise with increasing pressure as shown in Table 1 (Daage and Chianelli 1994). Calculations of *d*-spacing yield no discernible pattern across the samples (average of 6.30 Å). Using previously reported intensity ratio analysis (e.g., I_{110}:I_{002}), it was found that stacking was affected by a
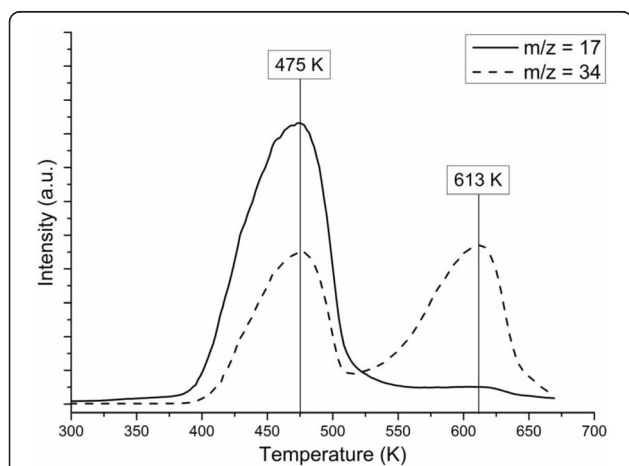
Figure 1 TPR-MS of reductive thermal decomposition of ATM. TPR-MS of reductive thermal decomposition of ATM under H_2 (5% H_2/He) showing evolution of NH_3 (m/z = 17) and H_2S (m/z = 34).

Figure 2 Change in specific surface area (S_{BET}) vs. decomposition time and H_2 pressure.

Whelan *et al. Journal of Analytical Science and Technology* (2015) 6:8

Page 4 of 8

Figure 3 Change in total pore volume (TPV) vs. decomposition time and H_2 pressure.

change in pressure and with time; using the Debye-Scherrer equation applied to the broadening of the (002) diffraction peak (Table 1), it was found that with increasing decomposition time and pressure the influence on stacking height decreased. However, of note is that while for 3 and 5 h increasing decomposition pressure increased stacking height, for the longest time in this study (7 h), stacking height was found to *decrease* as decomposition pressure increased. The exact role of stacking height on the catalytic activity of MoS_2 is unclear with support both for and against its influence (Daage and Chianelli 1994; Afanasiev 2010).

FT-IR catalyst characterization

Five distinct peaks were observed in the FT-IR spectra of the samples in the region below ca. 700 cm^{-1}: 655, 594, 462, 385, and 378 cm^{-1}. All samples were found to contain the first three peaks but varied in the latter two,
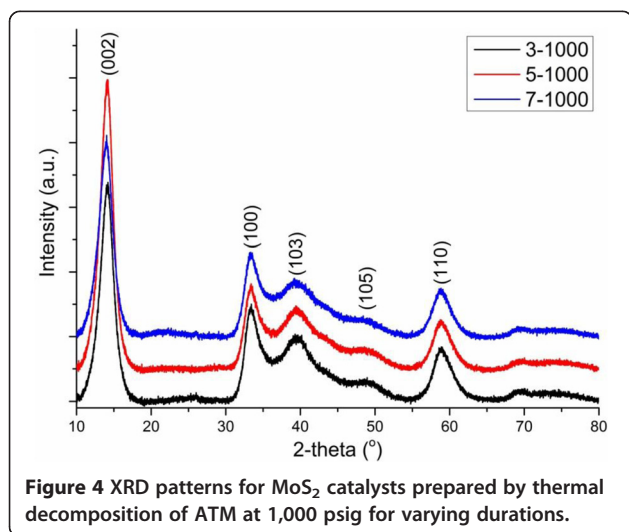
Figure 4 XRD patterns for MoS_2 catalysts prepared by thermal decomposition of ATM at 1,000 psig for varying durations.

containing 378 and/or 385 cm^{-1}. The FTIR spectra for MoS_2 catalysts prepared for 3-h decomposition time and 1,000 psig are shown in Figures 5 and 6, respectively (normalized against the peak at 378 cm^{-1} for ease of illustration). The peaks at 378 and 385 cm^{-1} have been assigned to Mo-S stretching vibrations along the basal plane (Berhault et al. 2002). With increasing heating time and pressure, the peak(s) at 378 and/or 385 cm^{-1} shifted towards a single peak at 378 cm^{-1}. The peak at 462 cm^{-1} is generally assigned to the Mo-S vibration perpendicular to the basal plane, i.e., the bridging Mo-S bond (Fedin et al. 1989). The presence of intermediate MoS_3 (with a peak at 385 cm^{-1}) is discounted due to the lack of corroborating peaks such as a peak at 525 cm^{-1} (Weber et al. 1995). The peaks at 655 and 594 cm^{-1} can be attributed to sulfur-containing peaks, with that at 655 cm^{-1} assigned to S-H vibrations (from Mo-SH) and that at 594 cm^{-1} attributed to S-S bonding strongly coupled to Mo-S (Müller et al. 1982).

Catalyst activity

HDS activity of each MoS_2 catalyst was tested, and the %DBT conversion of each catalyst is given in Table 2. HDS reaction conditions were set such that catalytic activity was kept below 20%, primarily to remove uncertainties associated with produced H_2S, which could limit the forward reaction and could increase the pressure in the batch reactor. A trend was observed of a general increase in HDS catalytic activity of MoS_2 prepared for longer decomposition times (i.e., across the row), with the exception of 7-*1,000*, as well as at higher H_2 pressure (i.e., down the column), excluding 7-*500* and 7-*1,000.* The amount of partial HYD is also given below (values in parentheses), and it can be seen that these percentages change depending upon the MoS_2 preparation conditions. As an example, the chromatogram of reaction product for 5-*500* showed a reduction of DBT (retention time = 20.4 min) concentration of 12.0% and an increase in HYD (retention time = 20.2 min) product of 2.8%; thus, direct desulfurization (DDS) accounts for 9.2% of DBT removal.

Diffusion rates of gaseous products from thermal decomposition of solids are known to decrease with an increase in pressure (Oyumi and Brill 1987). In the case of ATM decomposing, gas is released from each step (see Equations 1 and 2) leading to an increase in pressure which could slow down diffusion of gaseous by-products. This is expected to have an impact on the resulting MoS_2 formed.

Analysis of results

A general increase in S_{BET} with an increase in H_2 pressure (Figure 2) was observed across all decomposition times, though to varying degrees. The influence of decomposition time on S_{BET} at low pressure was minimal, though as

Whelan *et al. Journal of Analytical Science and Technology* (2015) 6:8

Page 5 of 8

Table 1 Crystalline order along the basal direction and apparent stacking heights in the *c*-axis direction

Pressure (psig)	20			500			1,000		
Time (h)	(110)	(002)	SA (m^2/g)	(110)	(002)	SA (m^2/g)	(110)	(002)	SA (m^2/g)
3	51	23	350	61	28	290	63	30	270
5	54	25	320	63	30	270	61	31	270
7	64	32	260	65	31	260	62	29	280

Crystalline order along the basal direction (Å) and apparent stacking heights in the *c*-axis direction (Å) calculated using the Debye-Scherrer equation to the broadening of the (110) and (002) diffraction peaks, respectively, for MoS2 catalysts. Surface Area (SA) was calculated in m^2/g using the formula mentioned in the work by Iwata et al (2001).

decomposition pressure increased, the influence of decomposition time became more pronounced. Based on the experimental parameters studied herein, it appears that 5 h was the optimal time and 1,000 psig the optimal pressure to produce a catalyst with the largest specific surface area. Increasing H$_2$ pressure was also found to produce larger pore volumes in the catalyst (Figure 3) leading to the conclusion that textural properties of the catalyst can be controlled by optimizing ATM decomposition time and pressure.

While increasing H$_2$ decomposition pressure increased S_{BET} within each decomposition time series, S_{BET} did not increase within each decomposition pressure series, particularly from 5 to 7 h. Intuitively, it is not unreasonable to expect an increase in pressure to result in a greater propensity for pore collapse (and subsequent decrease in surface area) which we see in 7-*500* and 7-*1,000*, when compared against 5-*500* and 5-*1,000*; however, the fact that pore collapse only happens at longer decomposition times again highlights the importance of the combined and sometimes conflicting roles of time and pressure and the necessity of varying ATM decomposition parameters to ensure greater control of the resulting MoS$_2$. A similar trend was observed for TPV of MoS$_2$ samples (Figure 3) in that the greatest increase in TPV was for the 5-h series and the lowest was for the 7-h series and likewise a

decrease in TPV for the high-pressure 7 h series compared to that for the 5-h series (e.g., compare 5-*500* with 7-*500* and 5-*1,000* with 7-*1,000*).

The change in stacking height with a change in pressure is not a novel concept having been noted before on supported hydrotreating catalysts, with HDS process conditions determined as the main cause of destacking (De la Rosa et al. 2004). Hydrothermal synthesis of MoS$_2$ in an autoclave was also found to result in destacking, and in that study, the presence of hydrocarbons was presented as a possible contributor (Peng et al. 2001) while, in a separate study, Chianelli et al. note that possible intercalation of H$_2$ at high pressures could result in MoS$_2$ layers simply sliding apart over time (Chianelli et al. 2006). However, all of these analyses were conducted on catalysts under HDS conditions whereas, in this case, stacking is not measured as a function of reaction conditions but as a function of thermal decomposition parameters on the original ATM starting material.

For any crystalline solid (in this case poorly crystalline), it can be expected that with an increase in stacking there should be a corresponding increase in S_{BET}; however, the degree to which S_{BET} increases would not be by the same factor as the increase in stacking, simply on the basis that it is only the exposed edge surface which will add to S_{BET} whereas the basal planes are 'covered' by the extra stacks
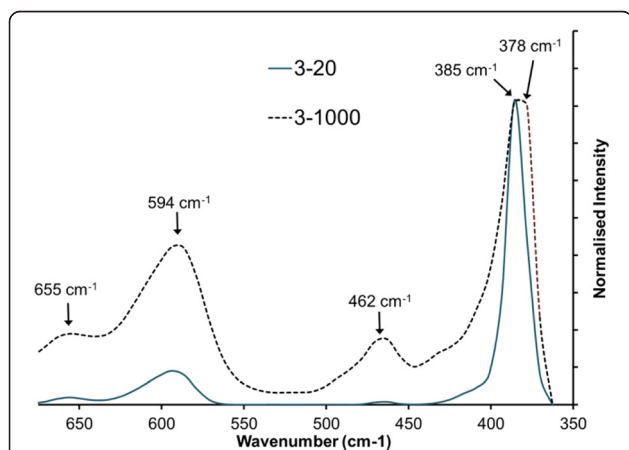
Figure 5 FT-IR spectra for specimens 3-*20* and 3-*1,000*. FT-IR spectra for specimens 3-*20* and 3-*1,000* showing variation of Mo-S peak vibrations (378 and/or 385 cm^{-1}) and S-S peak (592 cm^{-1}); spectra normalized against peak at 378 cm^{-1}.
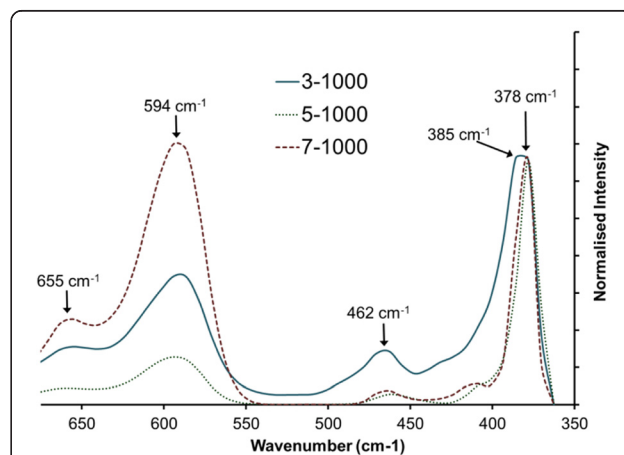
Figure 6 FT-IR spectra for 3-*1,000*, 5-*1,000* and 7-*1,000*. FT-IR spectra for 3-*1,000*, 5-*1,000*, and 7-*1,000* showing variation of Mo-S peak vibrations (378 and/or 385 cm^{-1}) and S-S peak (592 cm^{-1}); spectra normalized against peak at 378 cm^{-1}.

Whelan *et al. Journal of Analytical Science and Technology* (2015) 6:8

Page 6 of 8

Table 2 Catalytic activity of MoS$_2$ samples

Pressure (psig)	20	500	1,000
Time (h)			
3	1.7 (0)	5.8 (1.4)	12.0 (1.7)
5	5.8 (0)	12.0 (2.8)	15.0 (2.0)
7	7.7 (0)	10.0 (1.2)	5.2 (1.3)

Catalytic activity of MoS$_2$ samples defined as % conversion of DBT in hexadecane at 573 K, 500 psig (H$_2$), for 3 h. Values in parentheses represent the % of total conversion which is attributable to hydrogenated DBT (HYD).

(this of course infers perfect alignment of stacks). The use of S_{BET}, however, assumes that there is no agglomeration. Iwata et al. have observed vastly different S_{BET} from the theoretical values of surface area obtained from utilizing data from XRD (Iwata et al. 2001); applying their formula, a similar pattern is evident in our samples, i.e., agglomeration is occurring (compare Figure 2 and SA values in Table 1). While S_{BET} *increases* with an increase in decomposition pressure, it can be seen from Table 1 that the XRD-determined surface area *decreases*, appearing to level off close to 270 m^2 g^{-1}. Thus, the pattern emerges within each time series such that the extent of agglomeration is decreasing with an increase in decomposition pressure. Agglomeration is assumed to be prevalent in the solid state, i.e., during N$_2$ sorption, though less so during activity measurements due to the presence of solvent and high temperatures.
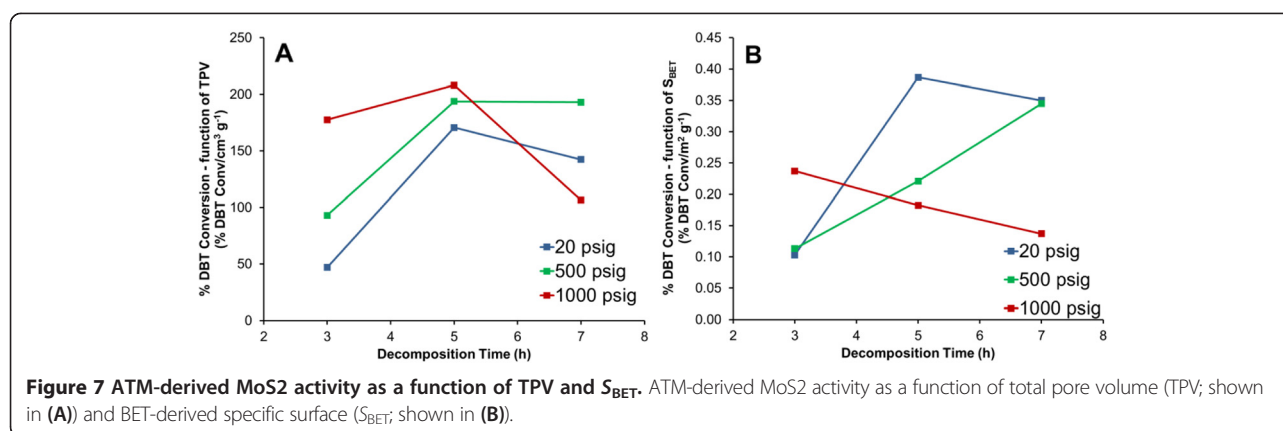
Previously reported modelling studies of poorly crystalline MoS$_2$ have shown that interlayer rotation about the *a*-axis results in little change for the 110 peak but in a shift of the 002 peak towards lower angles (Liang et al. 1986). The same authors model interlayer rotation about the *c*-axis, with changes observed in the 100-103-105 region, with only a small effect on the 002 and 110 peaks. XRD patterns of our samples display slight variations in the angle of 002, as well changes in I_{103}:I_{002} and I_{105}:I_{002} indicating interlayer rotation about the *a*- and *c*-axes, respectively, though by how much exactly is unknown.

The presence of two distinct peaks for Mo-S bonds implies a variation in strength and/or length; based on FT-IR vibrational energies, we assign 385 cm^{-1} to the stronger (i.e., shorter) Mo-S bond, with the weaker (longer) Mo-S bond at 378 cm^{-1}. Mo-S vibrations are usually assigned to the region ca. 380 cm^{-1}, with no literature evidence on FT-IR of MoS$_2$ found distinguishing between these peaks. In a related study, however, laser Raman studies of alumina-supported MoS$_2$ by Payen et al. observed a shift in the Raman band from 380 to 385 cm^{-1} with an increase in Mo loading (Payen et al. 1987); the authors attributed their shift (and broadening) to the lateral growth of MoS$_2$ particles without making reference to whether this 'crystallite size' effect is an actual broadening of the basal plane or merely side-to-side stacking of MoS$_2$ crystals. In our samples, it can be seen

that the crystallite sizes do increase with an increase in decomposition pressure though the values do not correlate well with the above conclusion - our results show a general increase in basal plane size but the results for 7-20 in particular and all samples prepared at 500 psig in general show similar crystalline orders than the samples prepared at 1,000 psig; thus at present, it is inconclusive that the peak shift is due (at least primarily) to lateral growth.

Since FT-IR spectra are of the bulk material, it could be argued that there is an increase in the concentration of weaker (longer), more reactive Mo-S bonds produced with increasing decomposition pressure. While this finding is intuitively unappealing as one would reasonably expect a shortening of bond lengths with increase in pressure (Pietosa et al. 2008), a possible explanation is that pressure induces structural changes which in turn induce creation of new catalytically active sites. Though recent investigations of MoS$_2$ nanoclusters using direct space DFT calculations have found that an increase in S atom coordination of Mo atom results in increasing Mo-S bond lengths (McBride and Head 2009), no such investigations were carried out in this study. Work is ongoing with a view to quantifying the interlayer rotations observed using XRD and the creation of new catalytically active sites and the unique FT-IR shifts observed through the preparation of more ATM-derived MoS$_2$ using more discreet changes in decomposition pressures.

One theory for the proposed catalytic activity of MoS$_2$ is that the presence of a coordinatively unsaturated site (CUS), with nearby SH groups, is a requirement for HDS (Lipsch and Schuit 1969). This CUS is formed by removal of sulfur from a molybdenum atom and occurs in the presence of H$_2$ (Alonso et al. 1998). Logically, therefore, the weaker the Mo-S bond the greater the concentration of sulfur vacancies that can be produced resulting in a higher activity (Nørskov et al. 1992). One can expect an improved HDS activity of MoS$_2$ with an FT-IR peak at 378 cm^{-1} over MoS$_2$ with a stronger Mo-S bond at 385 cm^{-1}, when comparing similar activity amongst catalysts of comparable texture and with the same strength of Mo-S peak. This was observed in the present study as well, with the exception of specimen 7-*1,000*, which exhibited different textural properties from other specimens. From the conditions under consideration in this study, all catalysts prepared at high pressure exhibited the weaker Mo-S bond and the largest S_{BET} and the largest TPV were found in 5-*1,000*; thus, it was surmised to be the best catalyst prepared for HDS of DBT. While 5-*1,000* did in fact have the highest activity in real terms (Table 2), as well as a function of TPV, it did not as a function of S_{BET} (Figure 7A,B, respectively). However, we have already shown that agglomeration occurs during S_{BET} measurements, so a more accurate representation would be to

Whelan *et al. Journal of Analytical Science and Technology* (2015) 6:8

Page 7 of 8

Figure 7 ATM-derived MoS2 activity as a function of TPV and S_{BET}. ATM-derived MoS2 activity as a function of total pore volume (TPV; shown in **(A)**) and BET-derived specific surface (S_{BET}; shown in **(B)**).

compare activity against the theoretically calculated surface area (from XRD). On this basis, 5-1,000 has the highest activity per unit area of MoS_2.

The increase in HYD:DDS ratio, as confirmed by chromatographic analysis, can be partially explained by a possible increase in the number of rim sites available due to interlayer rotation of the layers of MoS_2 in the stacks. Another possibility is that the reduced agglomeration from samples prepared at higher decomposition pressure simply exposes more rim sites to the DBT molecule. Of the samples which produce the hydrogenated DBT, 5-1,000 has one of the lowest HYD:DDS ratios (0.15) compared to say 3-500 (0.32). Thus, not only does 5-1,000 have a more active surface for HDS of DBT, but it also has a higher preference towards the DDS pathway compared to HYD which leads to the assumption that the exposure of rim sites for MoS_2 prepared from reductively decomposed ATM can be optimized by varying decomposition time and pressure.

Conclusions

We have shown herein the role played by both time and pressure for reductive thermal decomposition of ATM for the formation of MoS_2 and their subsequent impact on HDS activity. The influence of decomposition time serves to both enable an increase in surface area as well as an increased likelihood of sintering. Pressure increases slow down thermal decomposition by limiting gaseous by-product diffusion while at the same time facilitating the collapse of produced pores. Based on FT-IR vibrational energies, FT-IR spectral analysis shows that catalysts prepared at higher pressures have weaker Mo-S bonds (378 cm^{-1}) than those prepared at lower pressure (385 cm^{-1}). Evidence from XRD indicates both time and pressure induce interlayer rotation of stacks along both the *a*- and *c*-axes and that ATM decomposition pressure plays a role in determination of MoS_2 layer stacking. Using XRD-derived values for crystallite sizes, theoretical surface area values were determined; the

changes evident lead us to conclude that agglomeration is occurring. Optimal conditions were found producing a catalyst with weak Mo-S bonds, the largest (theoretical) surface area and largest pore volume which unsurprisingly resulted in the highest HDS activity of model dibenzothiophene. It was found that catalytic activity increased with a decrease in theoretical surface area, with 5-1,000 having the highest activity per unit area. Samples prepared at low pressures yielded no detectable HYD product, but this increased in samples prepared at higher decomposition pressure. An optimal system was found which gave the lowest HYD:DDS ratio, again 5-1,000. There is no doubt that there are other parameters which can impact both morphology and catalytic activity, such as ramp rates and variously substituted thiomolybdates; we have shown that the role of decomposition time and pressure for ATM-derived MoS_2 can in fact be a useful tool in optimizing catalyst synthesis with certain morphologies and activities.

Additional file

Additional file 1: XRD spectra from all synthesized MoS$_2$ catalysts. Figure S1. XRD patterns for MoS$_2$ catalysts prepared by thermal decomposition of ATM for 3 h at varying pressures. **Figure S2.** XRD patterns for MoS$_2$ catalysts prepared by thermal decomposition of ATM for 5 h at varying pressures. **Figure S3.** XRD patterns for MoS$_2$ catalysts prepared by thermal decomposition of ATM for 7 h at varying pressures.

Authors' contributions
JW: catalyst synthesis and characterization and manuscript writing; IB: catalyst testing; GEL: FTIR characterization; NDS: catalyst testing; SS: experimental design and execution; AT: XRD characterization; SAH: original idea and data interpretation; RVV: original idea and design of work; MSK: data interpretation and manuscript writing; SMA: overall supervision. All authors read and approved the final manuscript.

Whelan *et al. Journal of Analytical Science and Technology* (2015) 6:8

Page 8 of 8

Author details
[1]Department of Chemical Engineering, The Petroleum Institute, P.O. Box 2533, Abu Dhabi, United Arab Emirates. [2]Department of Chemistry, New York University Abu Dhabi, P.O. Box 129188, Abu Dhabi, UAE. [3]Department of Chemical and Biochemical Engineering, University Politehnica of Bucharest, 313 Spl. Independentei, sector 6, 060042, Bucharest, Romania. [4]Center for Organic Chemistry "C.D. Nenitzescu", 060023 Bucharest, Romania.

References

Afanasiev P (2008) Synthetic approaches to the molybdenum sulfide materials. Comptes Rendus Chimie 11(1–2):159–182, http://dx.doi.org/10.1016/j.crci.2007.04.009

Afanasiev P (2010) The influence of reducing and sulfiding conditions on the properties of unsupported MoS2-based catalysts. J Catal 269(2):269–280, http://dx.doi.org/10.1016/j.jcat.2009.11.004

Alekseevskii NE, Dobrovol'skii NM, Eckert D, Tsebro VI (1977) Investigation of critical currents of ternary molybdenum sulfides. J Low Temp Phys 29(5–6):565–572, doi:10.1007/bf00661547

Alonso G, Del Valle M, Cruz J, Petranovskii V, Licea-Claverie A, Fuentes S (1998) Preparation of MoS2 catalysts by in situ decomposition of tetraalkylammonium thiomolybdates. Catalysis Today 43(1–2):117–122, http://dx.doi.org/10.1016/S0920-5861(98)00140-0

Álvarez L, Berhault G, Alonso-Nuñez G (2008) Unsupported NiMo sulfide catalysts obtained from Nickel/Ammonium and Nickel/Tetraalkylammonium thiomolybdates: synthesis and application in the hydrodesulfurization of dibenzothiophene. Catal Lett 125(1–2):35–45, doi:10.1007/s10562-008-9541-2

Berhault G, Cota Araiza L, Duarte Moller A, Mehta A, Chianelli R (2002) Modifications of unpromoted and cobalt-promoted MoS2 during thermal treatment by dimethylsulfide. Catal Lett 78(1–4):81–90, doi:10.1023/a:1014910105975

Breysse M, Geantet C, Afanasiev P, Blanchard J, Vrinat M (2008) Recent studies on the preparation, activation and design of active phases and supports of hydrotreating catalysts. Catalysis Today 130(1):3–13, http://dx.doi.org/10.1016/j.cattod.2007.08.018

Brunet S, Mey D, Pérot G, Bouchy C, Diehl F (2005) On the hydrodesulfurization of FCC gasoline: a review. Appl Catal Gen 278(2):143–172, http://dx.doi.org/10.1016/j.apcata.2004.10.012

Camacho-Bragado GA, Elechiguerra JL, Olivas A, Fuentes S, Galvan D, Yacaman MJ (2005) Structure and catalytic properties of nanostructured molybdenum sulfides. J Catal 234(1):182–190, http://dx.doi.org/10.1016/j.jcat.2005.06.009

Chianelli RR, Siadati MH, De la Rosa MP, Berhault G, Wilcoxon JP, Bearden R, Abrams BL (2006) Catalytic properties of single layers of transition metal sulfide catalytic materials. Catalysis Rev 48(1):1–41, doi:10.1080/01614940500439776

Chianelli RR, Berhault G, Torres B (2009) Unsupported transition metal sulfide catalysts: 100 years of science and application. Catalysis Today 147(3–4):275–286, http://dx.doi.org/10.1016/j.cattod.2008.09.041

Criado J, González M, Málek J, Ortega A (1995) The effect of the CO2 pressure on the thermal decomposition kinetics of calcium carbonate. Thermochimica Acta 254(0):121–127, http://dx.doi.org/10.1016/0040-6031(94)01998-V

Daage M, Chianelli RR (1994) Structure-function relations in molybdenum sulfide catalysts: the "Rim-Edge" model. J Catal 149(2):414–427, http://dx.doi.org/10.1006/jcat.1994.1308

De la Rosa MP, Texier S, Berhault G, Camacho A, Yácaman MJ, Mehta A, Fuentes S, Montoya JA, Murrieta F, Chianelli RR (2004) Structural studies of catalytically stabilized model and industrial-supported hydrodesulfurization catalysts. J Catal 225(2):288–299, http://dx.doi.org/10.1016/j.jcat.2004.03.039

Devers E, Afanasiev P, Jouguet B, Vrinat M (2002) Hydrothermal syntheses and catalytic properties of dispersed molybdenum sulfides. Catal Lett 82(1–2):13–17, doi:10.1023/a:1020512320773

Egorova M, Prins R (2006) The role of Ni and Co promoters in the simultaneous HDS of dibenzothiophene and HDN of amines over Mo/γ-Al2O3 catalysts. J Catal 241(1):162–172, http://dx.doi.org/10.1016/j.jcat.2006.04.011

Fedin VP, Kolesov BA, Mironov YV, Fedorov VY (1989) Synthesis and vibrational (IR and Raman) spectroscopic study of triangular thio-complexes [Mo3S13]2− containing 92Mo, 100Mo and 34S isotopes. Polyhedron 8(20):2419–2423, http://dx.doi.org/10.1016/S0277-5387(89)80005-1

Iwata Y, Araki Y, Honna K, Miki Y, Sato K, Shimada H (2001) Hydrogenation active sites of unsupported molybdenum sulfide catalysts for hydroprocessing heavy oils. Catalysis Today 65(2–4):335–341, http://dx.doi.org/10.1016/S0920-5861(00)00554-X

Klimov OV, Pashigreva AV, Fedotov MA, Kochubey DI, Chesalov YA, Bukhtiyarova GA, Noskov AS (2010) Co–Mo catalysts for ultra-deep HDS of diesel fuels prepared via synthesis of bimetallic surface compounds. J Mol Catalysis A Chem 322(1–2):80–89, http://dx.doi.org/10.1016/j.molcata.2010.02.020

Liang KS, Chianelli RR, Chien FZ, Moss SC (1986) Structure of poorly crystalline MoS2 — a modeling study. J Non Cryst Solids 79(3):251–273, http://dx.doi.org/10.1016/0022-3093(86)90226-7

Lipsch JMJG, Schuit GCA (1969) The CoO MoO3 Al2O3 catalyst: III. Catalytic properties. J Catal 15(2):179–189, http://dx.doi.org/10.1016/0021-9517(69)90022-0

McBride KL, Head JD (2009) DFT investigation of MoS2 nanoclusters used as desulfurization catalysts. Int J Quantum Chem 109(15):3570–3582, doi:10.1002/qua.22328

Mdleleni MM, Hyeon T, Suslick KS (1998) Sonochemical synthesis of nanostructured molybdenum sulfide. J Am Chem Soc 120(24):6189–6190, doi:10.1021/ja9800333

Müller A, Jaegermann W, Enemark JH (1982) Disulfur complexes. Coord Chem Rev 46:245–280

Nørskov JK, Clausen BS, Topsøe H (1992) Understanding the trends in the hydrodesulfurization activity of the transition metal sulfides. Catal Lett 13(1–2):1–8, doi:10.1007/bf00770941

Oyumi Y, Brill TB (1987) Thermal decomposition of energetic materials 22. The contrasting effects of pressure on the high-rate thermolysis of 34 energetic compounds. Combustion Flame 68(2):209–216, http://dx.doi.org/10.1016/0010-2180(87)90058-7

Payen E, Grimblot J, Kasztelan S (1987) Study of oxidic and reduced alumina-supported molybdate and heptamolybdate species by in situ laser Raman spectroscopy. J Phys Chem 91(27):6642–6648, doi:10.1021/j100311a018

Peng Y, Meng Z, Zhong C, Lu J, Yu W, Yang Z, Qian Y (2001) Hydrothermal synthesis of MoS2 and its pressure-related crystallization. J Solid State Chem 159(1):170–173, http://dx.doi.org/10.1006/jssc.2001.9146

Piermarini GJ, Block S, Miller PJ (1987) Effects of pressure and temperature on the thermal decomposition rate and reaction mechanism of.beta.-octahydro-1,3,5,7-tetranitro-1,3,5,7-tetrazocine. J Phys Chem 91(14):3872–3878, doi:10.1021/j100298a028

Pietosa J, Dabrowski B, Wisniewski A, Puzniak R, Kiyanagi R, Maxwell T, Jorgensen JD (2008) Pressure effects on magnetic and structural properties of pure and substituted SrRuO3. Phys Rev B 77(10):104410

Polyakov M, van den Berg MWE, Hanft T, Poisot M, Bensch W, Muhler M, Grünert W (2008) Hydrocarbon reactions on MoS2 revisited, I: activation of MoS2 and interaction with hydrogen studied by transient kinetic experiments. J Catal 256(1):126–136, http://dx.doi.org/10.1016/j.jcat.2008.03.007

Sánchez V, Benavente E, Lavayen V, O'Dwyer C, Sotomayor Torres CM, González G, Santa Ana MA (2006) Pressure induced anisotropy of electrical conductivity in polycrystalline molybdenum disulfide. Appl Surf Sci 252 (22):7941–7947, http://dx.doi.org/10.1016/j.apsusc.2005.10.011

Topsøe H, Clausen B, Massoth F (1996) Hydrotreating catalysis. In: Anderson J, Boudart M (eds) Catalysis, vol 11, Catalysis-science and technology. Springer, Berlin Heidelberg, pp 1–269, doi:10.1007/978-3-642-61040-0_1

Walton RI, Dent AJ, Hibble SJ (1998) In situ investigation of the thermal decomposition of ammonium tetrathiomolybdate using combined time-resolved X-ray absorption spectroscopy and X-ray diffraction. Chem Mater 10(11):3737–3745, doi:10.1021/cm980716h

Weber T, Muijsers JC, Niemantsverdriet JW (1995) Structure of amorphous MoS3. J Phys Chem 99(22):9194–9200, doi:10.1021/j100022a037

Zhang F, Vasudevan PT (1995) TPD and HYD studies of unpromoted and co-promoted molybdenum sulfide catalyst ex ammonium tetrathiomolybdate. J Catal 157 (2):536–544, http://dx.doi.org/10.1006/jcat.1995.1317